

Effects of Certain Design Parameters on Load/Unload Performance

Qing-Hua Zeng and David B. Bogy

Computer Mechanics Laboratory
Department of Mechanical Engineering
University of California
Berkeley, CA 94720

ABSTRACT

Dynamic load/unload (L/UL) has been widely used in portable and removable drives, and the disk drive industry has started to apply it in desktop and server drives. There are many design parameters in L/UL systems. In this paper, we focus on the effects of the ramp profile, slider burnish, disk RPM, loading velocity, and dimple pre-load on L/UL performance. Our simulation results show that the loading process is much smoother at low RPM, slider burnish increases the steady flying attitudes and slightly smoothens the L/UL process. The loading velocity effects are not significant in a wide velocity range for negative pressure sliders. Properly designed ramps can obviously improve the unloading performance, and specially designed ramp profiles can also improve the loading performance at high velocity loading. A larger dimple pre-load can suppress the pitch oscillation during loading.

I. INTRODUCTION

Dynamic load/unload (L/UL) has been widely used in portable and removable drives. The disk drive industry has started to apply it in desktop and server drives to avoid slider-disk stiction and wear problems. The main design objectives of L/UL mechanisms are no slider-disk contact or no media damage even with contact during L/UL, and a smooth and short unloading process. Jeong and Bogy [1], Fu and Bogy [2] studied L/UL systems by experiments to find the conditions for avoiding slider-disk contacts. Suk and Gillis [3] experimentally researched the effect of slider burnish on disk damage during L/UL, and found that a properly burnished slider rarely causes any disk damage and improves the reliability. Jeong and Bogy [4] and Hu [5] simulated the loading process and showed that squeeze flow effects play an important role during the loading process. Almost all current drives use negative pressure sliders, so Zeng et. al. [6] and Hu et. al. [7] investigated the unloading process of negative pressure sliders, and they showed that the suction forces result in severe problems for most current sliders during unload. To prevent these problems, Zeng and Bogy [8] designed sliders specifically for L/UL applications thereby achieving the preferred performance. Another approach, specifically designed suspensions with limiters, is also currently employed in the industry, so Zeng and Bogy [9] investigated the effects of the limiters on the L/UL processes, and found that properly designed limiters can greatly improve the unloading performance. We also presented a new 4-DOF suspension model for L/UL simulation and applied it to simulate the L/UL process of a pico slider that was used in recent IBM mobile drives [10]. The results showed that the unloading process can be accurately simulated by using this model, and the loading process can be more accurately simulated by using this 4-DOF model than other models [5]-[7]. Chapin and Bogy [11] built a new

experimental apparatus and measured the air bearing forces of pico sliders during unloading. The measured data are very useful for quantitatively verifying the simulation model and results.

In a L/UL system there are many design parameters, such as the L/UL parameters, the slider air bearing designs, and the suspension parameters. A better understanding of the effects of all these parameters is very important for design. In this paper, we focus on the effects of several parameters of the L/UL process, such as the ramp profile, slider burnish, disk RPM, loading velocity, and dimple pre-load. These aspects have not previously been well researched. Our simulation results show that the loading process is much smoother at low RPM, slider burnish increases the steady flying attitudes and slightly smoothens the L/UL process. The loading velocity effects are not significant in a very wide velocity range for negative pressure sliders. Properly designed ramps can obviously improve the unloading performance, and specially designed ramp profiles can also improve the loading performance at high velocity loading. A larger dimple pre-load can suppress pitch oscillation during loading, which can also eliminate slider-disk contacts.

II. MATHEMATICAL MODELS

The mathematical models used in this paper are similar to those used in our paper [10]. The air bearing slider is attached to a suspension. Because of the constraints of the suspension, the slider's motion can be described as a system with three degrees of freedom (DOFs). There are four kinds of forces and moments applied on the slider. The first is the air bearing force and moments that are governed by the generalized Reynolds equation. The second is the asperity contact force and moments, which are calculated by the Greenwood-Williamson method if the

flying height (FH) is less than the glide height. The third is the impact force and moments calculated by the elastic-plastic model if the FH is less than zero (i.e., slider indentation of the disk). The fourth is the suspension force and moments that are calculated from the equation

$$\begin{bmatrix} F_L \\ F_S \\ M_{S\theta} \\ M_{S\beta} \end{bmatrix} = -[K_j]_{4 \times 4} \begin{bmatrix} z_L \\ z \\ \theta \\ \beta \end{bmatrix} - \begin{bmatrix} 0 \\ c_z \dot{z} \\ c_\theta \dot{\theta} \\ c_\beta \dot{\beta} \end{bmatrix} \quad (1)$$

where F_L is the force applied by the ramp, F_S is the suspension force applied on the slider's center, and $M_{S\theta}$ and $M_{S\beta}$ are suspension moments in the pitch and roll direction. z , θ and β are the vertical displacement at the slider's center, and the slider's pitch and roll. c_z , c_θ , and c_β are damping coefficients of the suspension in the vertical, pitch and roll directions. z_L is the displacement at the L/UL tab. There are several states of the suspensions in the L/UL process based on the contact conditions at the loading dimple, limiters and ramp. There are four states for the suspensions with a dimple and limiters if the limiters are closed or separate at the same time. In each state, we have a different 4×4 stiffness matrix $[K_j]$, which is calculated from FE models. The effects of suspension inertia are included in the slider's inertia moments calculated by combining the calculated stiffness and the measured modal frequencies.

III. SIMULATION RESULTS AND DISCUSSIONS

Two 30% (1.2×1.0 mm) sliders (A and B) and a suspension that were used by Zeng and Bogy [9] are also used here. The sliders' air bearings are shown in Fig. 1. The suspension has a dimple and two limiters. The two sliders have almost a uniform 30 nm flying height from the ID (21.2 mm, -7.5°) to the OD (45 mm, 16°) at 7200 RPM, and are loaded/unloaded at the OD.

A. The effects of disk RPM on the loading process.

Because the disk RPM can be easily specified during the loading process, we simulated the effect of the disk RPM on loading performance for the two sliders. The sliders are loaded at a vertical velocity of 25.4 mm/s at different disk RPM. Figures 2 and 3 show the pitch and minimum clearance histories of the sliders loaded at different RPM. The initial pitch is less than zero because of the geometrical effects of the initial displacement (20 μm) of the L/UL tab. All of the minimum values of the minimum clearances in Fig. 2 are larger than zero. That means no contact occurs between the disk and the slider A. All of these values in Fig. 3 are negative indicating that slider B contacts the disk during loading.

From Figs. 2 and 3, it can be seen that slider A has a smoother loading process than slider B, and the process is much smoother at the low RPM. Figure 4 shows the air bearing forces and the force center in the initial loading stage of the sliders. The two sliders have quite different air bearing force histories. The air bearing of slider A is smoothly and gradually built up. During the entire loading process, the negative pressure (suction) force is located between the slider's center and the trailing edge, and this results in a positive pitch moment. In the initial stage, the positive pressure (lift) force center is between the slider's center and the leading edge, and it also generates a positive pitch moment. Therefore, the pitch increases as the air bearing forces build up during loading. When the pitch increases the center of the lift force approaches the trailing edge, the positive moment decreases, and the pitch decreases. Thus, pitch oscillations occur. At higher RPM, there are larger lift forces, so there are stronger oscillations. The suction force always generates a positive pitch moment for slider A, so it can be smoothly loaded at different RPM.

For slider B, the suction force is located between the slider's center and the leading edge, and this results in a negative pitch moment during the entire loading process. In the initial stage (near 0.5 ms range), the lift force center is between the slider's center and leading edge, and it also generates a positive pitch moment. However, this positive moment is smaller than the negative moment because of the smaller lift force. Therefore, the pitch decreases as the air bearing develops. When the pitch decreases, the center of the suction force approaches the leading edge, the negative moment increases, and the pitch decreases further. This results in slider-disk contacts. Then, the lift force increases quickly, and its center rapidly approaches the leading edge. So, the positive moment increases dramatically. This moment plus the contact and impact force effects result in a sharply increasing pitch. When the pitch increases, the center of the lift force moves to the trailing edge and generates a negative moment. At this point (about 0.57 ms), both the lift and suction forces generate the negative moment, and the pitch quickly decreases. Thus, strong pitch oscillations occur. At higher RPM, the lift and suction forces are larger, and therefore the oscillations become stronger.

If the loading velocity is increased to 50.8 mm/s, the results show no obvious change. However, if a 0.5 degrees PSA is imposed, the loading performance is greatly improved, as shown in Fig. 5. That is because the positive PSA generates a positive pitch moment and increases the pitch. Figure 5 also clearly shows that the lower the RPM, the smoother the loading process. All of the results show that both sliders have a better loading performance at lower RPM. These two sliders are two extreme designs, and the loading performances of most current negative pressure sliders are expected to be between them. Therefore, it is strongly suggested that all negative pressure sliders should be loaded at lower disk RPM.

B. The effects of the loading velocity.

The published results [4, 5] showed that the loading velocity significantly affects the loading process. The loading processes of the two sliders were simulated for the different vertical loading velocities at 7200 RPM, 0 PSA. Higher acceleration (300 m/s^2) and initial FH ($30 \text{ }\mu\text{m}$) were used to achieve the given velocities, which are in a wide range of 12.7 to 101.6 mm/s, before the air bearing appears. The simulation results (Fig. 6) show that the velocity effects are not significant in this velocity range. Slider A doesn't contact the disk, and slider B contacts the disk in all five cases. Slider B strongly hits the disk two times at 12.7 mm/s and three times at 101.6 mm/s, and it slightly touches the disk at 50.8 mm/s. Therefore, slider B has a better loading performance at the medium velocity, such as 50.8 mm/s. Slider A has a smoother loading process at the higher velocity, as shown in Fig. 6 a).

C. The effects of slider burnish.

Experimental results [3] show that slider burnish significantly affects the loading process. Simulation work is definitely required to better understand the effects of slider burnish. Based on the parameters presented in [3], we changed the wall profiles of the small rail and the outer sides of slider B to model the slider burnish, and kept all other parameters unchanged. Figure 7 shows two of the wall profiles used in simulation representing different stages of burnish. The rail shapes of the slider before and after burnished are shown in Fig. 8. To better model the effect of the wall profiles, and simulate the loading process, we manually defined the grids. The total grid size is 273×225 , and the same grids were used in both the un-burnished and the burnished sliders. First, the steady flying attitudes were calculated and are shown in Table 1. It can be seen that the

burnish greatly increases the flying attitudes. That is because the wall profiles of the burnished slider work as small tapers, and cause the air pressure to build-up at the leading edge of the slider and the front of the small pad.

Next, the unloading performance was calculated. The results indicate that the slider burnish decreases the lift-off force from 18.71 mN to 17.96 mN when it is unloaded at 100 mm/s, thereby slightly improving the unloading performance. However, generally speaking, the slider burnish doesn't significantly affect the unload performance. Finally, the loading performance was evaluated. Figure 9 shows the slider's pitch and the minimum clearance of the burnished and un-burnished sliders when they are loaded at 25.4 mm/s. If the PSA is 0, the un-burnished slider hits the disk, while the burnished slider doesn't. If the PSA is -0.5 degree, the un-burnished slider strongly hits the disk several times, and the process is not smooth. However, the burnished slider hits the disk only one time, and is quickly loaded. Therefore, the slider burnish changes the slider's air bearing surfaces, and slightly improves the L/UL performance. It seems that the main effect of the burnish is to reduce the stress when the slider hits the disk and thereby reducing the disk damage, as explained in [3].

D. The effects of the ramp profile.

It is possible to improve the L/UL performance by changing the L/UL vertical velocity in the L/UL process. The vertical velocity is determined by the actuator velocity and the ramp profile. It is not easy to precisely control the actuator velocity, especially during unloading. Therefore, we assume the actuator velocity is constant in the track seeking direction, then the vertical L/UL velocity can be changed by changing the ramp profile. Slider A has good L/UL performance, and

it doesn't need a special ramp profile. We therefore designed ramp profiles to improve slider B's L/UL performance.

Avoiding slider/disk contact, decreasing the ramp force, and shortening the unloading process are preferred for slider B. If the negative pressure sliders are unloaded, contact may occur at two stages. The first stage is when the air bearing exists and the suspension dimple separates if the ABS and/or suspension are not properly designed [8,9], or the vertical unloading velocity is very large. This can be avoided by changing the ABS and/or suspension design, and limiting the velocity. The second stage is after the air bearing disappears, the dimple closes, and the slider strongly rebounds and then hits the disk. This can be avoided by decreasing the lift-off forces and increasing the unloading velocity. However, increasing the velocity will increase the lift-off force [10]. This conflicted requirement can be satisfied if the ramp profile is properly designed. We designed the ramp to have a small slope at the low height, at which the air bearing exists. We achieve a low velocity and thereby a small lift-off force. The ramp has a larger slope at the higher height, at which the air bearing disappears. We achieve a high unloading velocity to move the slider away.

Slider B is unloaded at an 80 mm/s horizontal velocity with ramp A that has a 15 degrees uniform slope. The force histories are shown in Fig 10. The lift-off force is 15.76 mN, and the maximum ramp force is 29.76 mN. The air bearing breaks at about 4.5 ms. Figure 11 shows the displacement and the minimum clearance between the slider and the disk. We can see that the slider almost hits the disk at about 4.8 ms after the air bearing disappears and the slider rebounds.

The minimum clearance is $0.356\ \mu\text{m}$ at this point. The unloading process is finished in a 6 ms period. The effective ramp height and length are $480\ \mu\text{m}$ and $128.62\ \mu\text{m}$.

To improve the unloading performance we designed three ramp profiles and simulated the unloading process of slider B with these ramps. The ramp profiles and the unloading performances are shown in Fig. 11 and Table 2. The three ramps have the same effective ramp height and length as ramp A. Ramp B has two regions with different slopes. One slope is 13.21 degrees with a $411\ \mu\text{m}$ length ($0\sim 5.139$ ms), and the other is 25 degrees with a $68.88\ \mu\text{m}$ length. Ramp C has three regions with slopes of 15 , 6.78 , and 25 degrees. Ramp D has two regions. One has a 12.77 degrees slope and a $422.5\ \mu\text{m}$ length ($0\sim 5.29$ ms), and the other has a 30 degrees slope and a $56.5\ \mu\text{m}$ length. These three ramps significantly increase the minimum clearances from $0.356\ \mu\text{m}$ to 5.80 , 4.92 and $10.38\ \mu\text{m}$, respectively, after the air bearing disappears, and slightly decrease the ramp force from 29.76 mN to 29.51 , 28.92 , and 29.74 mN, respectively. Therefore, all three ramp designs have better unloading performance than ramp A, and they can prevent the slider hitting the disk.

There are only small differences in the loading performance for the four ramp profiles that are specially designed for improving the unloading performance of slider B. That is because the ramp profiles change the loading velocity, but the loading velocity has no significant effect on the loading process of slider B in a wide velocity range as shown in Fig 6. However, we can also specially design the ramp profiles to improve the loading performance at high speed loading. Figure 12 shows the loading process of slider B unloaded at a $300\ \text{mm/s}$ horizontal velocity with ramps A and E. It is observed that ramp E has a better loading performance.

For unloading, the key to the ramp profile design is finding the point at which the air bearing breaks. Below this point, the ramp should have a small slope, and the ramp has a larger slope above this point. For loading, we need to find the point at which the air bearing quickly builds up. Above this point, the ramp has a large slope, and the ramp has a small slope below this point. The required trend of the ramp slope is the same for both loading and unloading. However, these two points are at different heights for most negative pressure sliders and suspension systems. Therefore, we specially designed ramp F, as shown in Fig. 13, to improve both loading and unloading performances. This ramp has a similar unloading performance as ramp D, and a better loading performance than ramps A-D.

E. The effects of dimple pre-load.

Figure 13 also shows the effect of dimple pre-load on the loading process of slider B with ramp E. There is a large pitch oscillation. That is because the change of the slope of the ramp from 0 degree to 30 degrees causes a small excitation to be applied to the slider. The slider oscillates, and the dimple separates. After the dimple separates, the suspension force moves to the leading edge, and it generates a larger pitch moment [7]. This moment results in the pitch oscillation. If the dimple pre-load is increased from 0.1 mN to 1.5 mN, the dimple separation is prevented, and the pitch oscillation is significantly decreased, as shown in Fig. 13. Therefore, a larger dimple pre-load smoothens the loading process. Smoothing the ramp can also decrease the oscillation.

IV. CONCLUSION

The mathematical models used in the L/UL simulation are briefly discussed, and then we focus on the effects of several parameters on the L/UL process, such as the ramp profile, slider burnish, disk RPM, and loading velocity. Two negative pressure pico sliders attached to a TSA suspension with limiters were used in the simulations. The results show that the loading process is much smoother at low RPM. Therefore, it is strongly suggested that all negative pressure sliders be loaded at lower disk RPM. Slider burnish increases the steady flying attitudes and slightly smoothens the L/UL process. The loading velocity effects are not significant in a very wide velocity range for the negative pressure sliders. Properly designed ramps can obviously improve the unloading performance, and specially designed ramp profiles can also improve the loading performance at high velocity loading. A larger dimple pre-load can suppress the pitch oscillation during loading.

ACKNOWLEDGMENTS

This study is supported by the Computer Mechanics Laboratory at the University of California at Berkeley.

REFERENCES

- [1] T. G. Jeong and D. B. Bogy, "An experimental study of the parameters that determine slider-disk contacts during dynamic load-unload," *ASME Journal of Tribology*, Vol. 114, pp. 507-514, 1992.

- [2] T. C. Fu and D. B. Bogy, "Slider-disk contacts during the loading process in a ramp-load magnetic disk drive," *Adv. Info. Storage Syst.*, Vol. 6, pp. 41-54, 1995.
- [3] M. Suk and D. Gillis, "Effects of slider burnish on disk damage during dynamic load/unload," *ASME J. of Trib.*, Vol. 120, pp. 332-338, 1998.
- [4] T. G. Jeong and D. B. Bogy, "Numerical simulation of dynamic loading in hard disk drives," *ASME J. of Trib.*, Vol. 115, pp. 370-375, 1993.
- [5] Y. Hu, "Ramp-Load Dynamics of Proximity Recording Air Bearing Sliders in Magnetic Hard Disk Drive," ASME/STLE, International Tribology Conference, Toronto, Canada, Oct. 25-28, 1998.
- [6] Q. H. Zeng, M. Chapin and D. B. Bogy, "Dynamics of the unload process for negative pressure sliders," *IEEE Trans. Magn.*, Vol. 35, pp. 916-920, 1999.
- [7] Y. Hu, P. M. Jones and K. Li, "Air bearing dynamics of sub-ambient pressure sliders during dynamic unload," ASME/STLE, International Tribology Conference, Toronto, Canada, Oct. 25-28, 1998.
- [8] Q. H. Zeng and D. B. Bogy, "Slider air bearing designs for load/unload applications," *IEEE Trans. Magn.*, Vol. 35, pp. 746-751, 1999.
- [9] Q. H. Zeng and D. B. Bogy, "Effects of Suspension Limiters on the Dynamic Load/Unload Process: Numerical Simulation," *IEEE Trans. Magn.*, Vol.35, Sept. 1999, in press.
- [10] Q. H. Zeng and D. B. Bogy, "A Simplified 4-DOF Suspension Model for Dynamic Load/Unload Simulation and its Application," *ASME Journal of Tribology*, in press.
- [11] M. Chapin and D. B. Bogy, "Air Bearing Force Measurement of Pico Negative Pressure Sliders During Dynamic Unload," *ASME Journal of Tribology*, in press.

TABLE 1

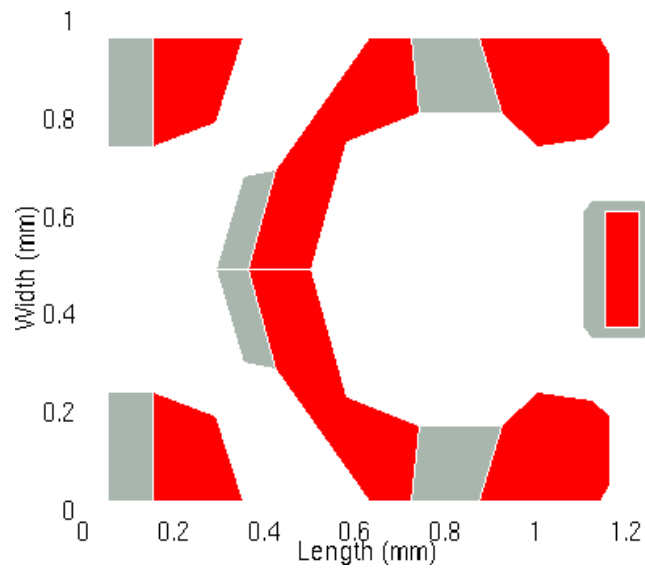
STEADY FLYING ATTITUDES OF UN-BURNISHED AND BURNISHED SLIDERS

Sliders	Nominal FH (nm)	Pitch (urad)	Roll (urad)
Un-burnished	25.31	76.23	1.80
Burnished	39.34	98.01	-11.5

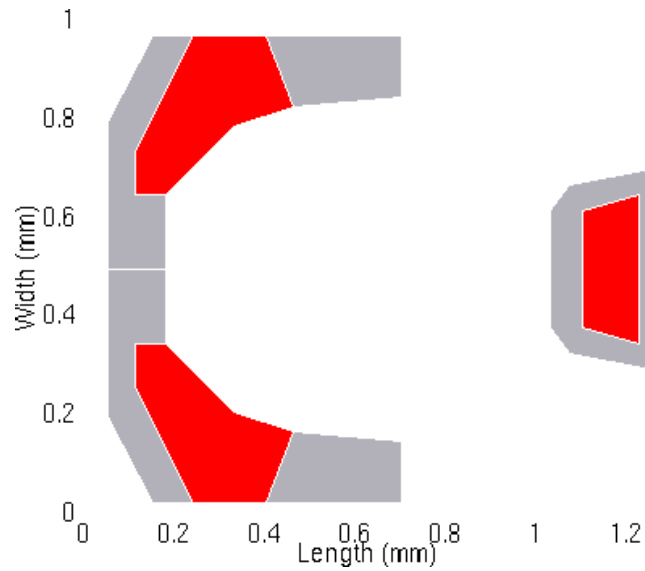
TABLE 2

UNLOADING PERFORMANCE OF SLIDER A FOR THE FOUR RAMPS

Ramp	A	B	C	D
Ramp slop (degree)	15	13.2	15	12.77
		25	6.78	30
			25	
Lift-off force (mN)	15.76	15.60	14.95	15.56
Maximum ramp force (mN)	29.76	29.51	28.92	29.74
Minimum clearance (μm)	0.356	5.80	4.919	10.38



a) Slider A



b) Slider B

Fig. 1 Two sliders

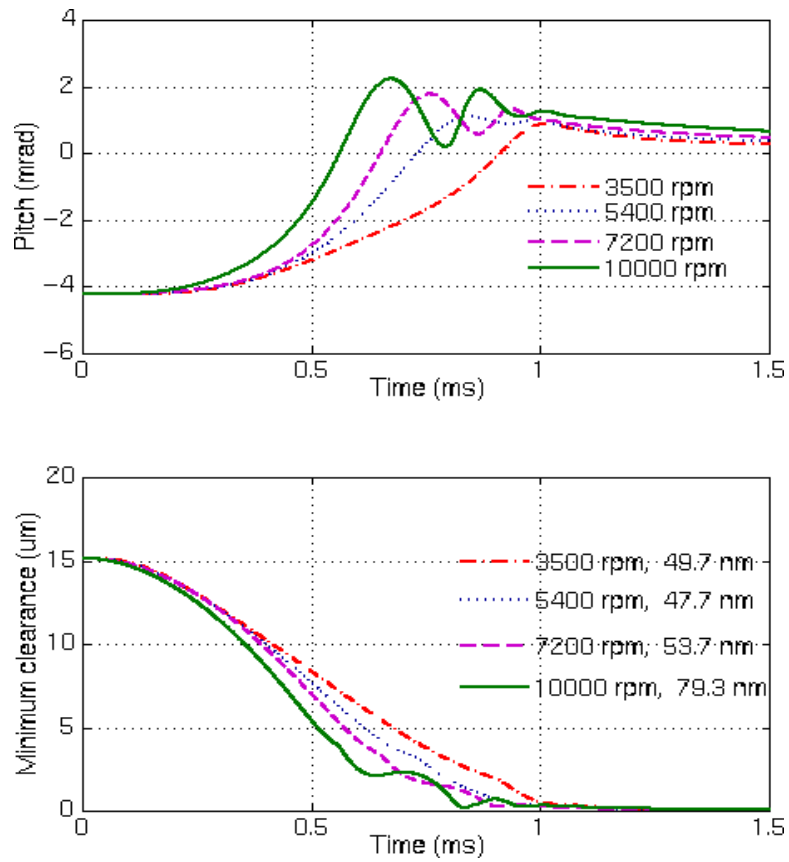


Fig. 2 Slider A's pitch and minimum clearance history during the loading process at different disk RPM (PSA=0 degree).

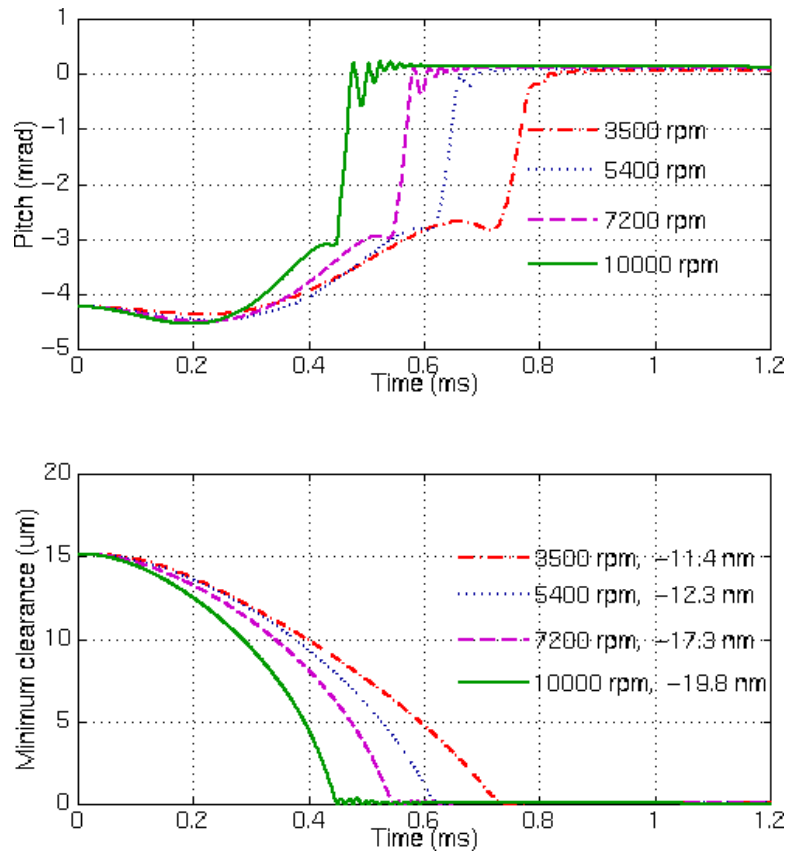


Fig. 3 Slider B's pitch and minimum clearance history for different disk RPM (PSA=0 degree).

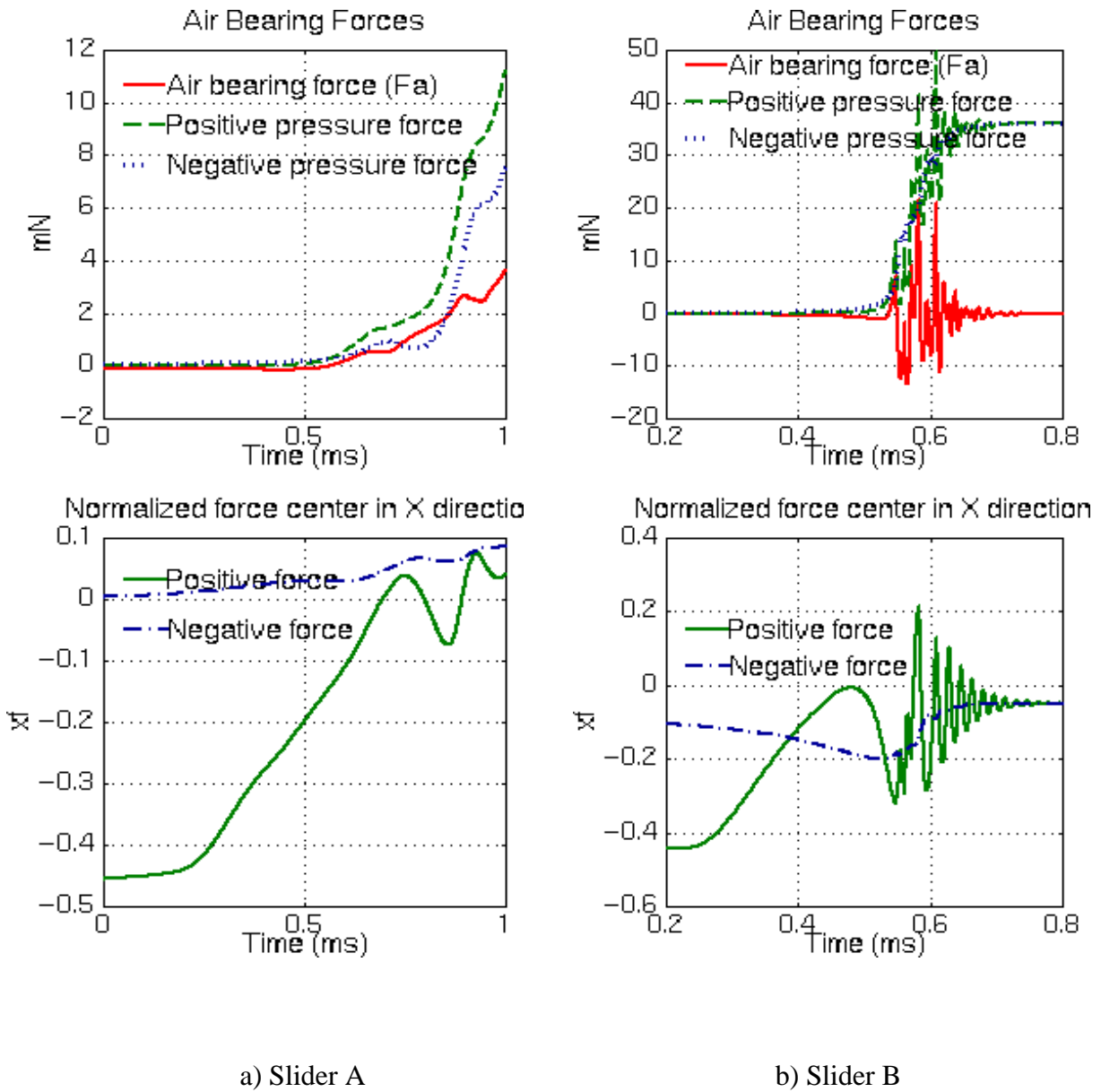


Fig. 4 Air bearing forces and force center in the initial stage of the loading process of the two sliders. The force center $xf=0.5$ means the force center is at the leading edge of the sliders, and -0.5 is at the trailing edge.

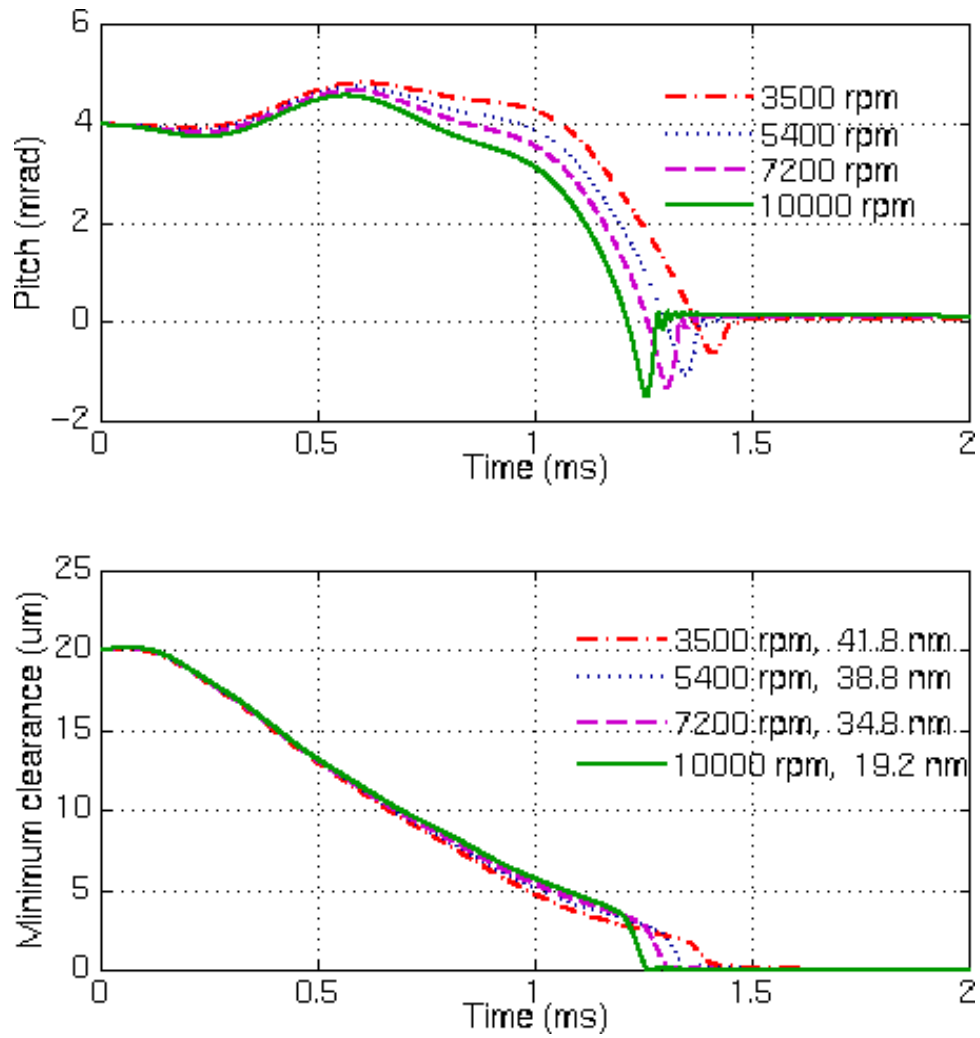
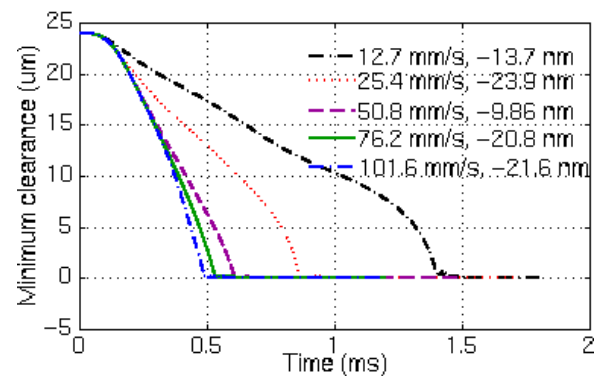
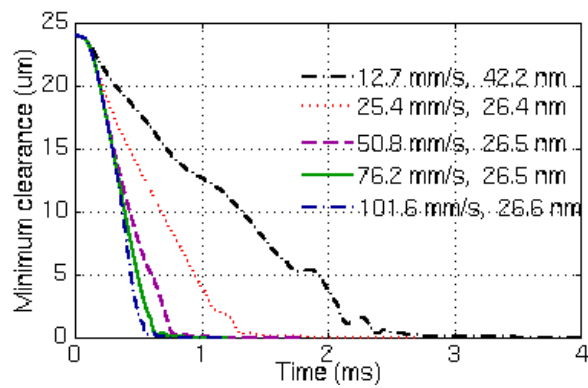
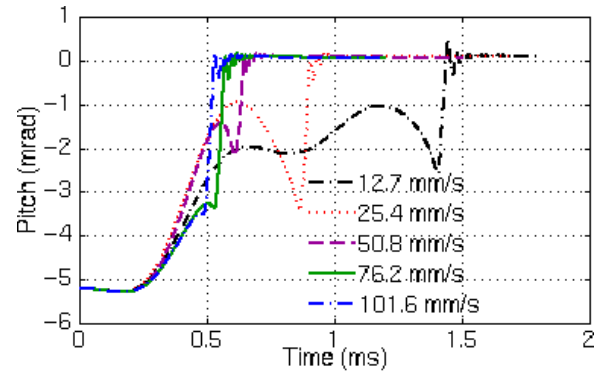
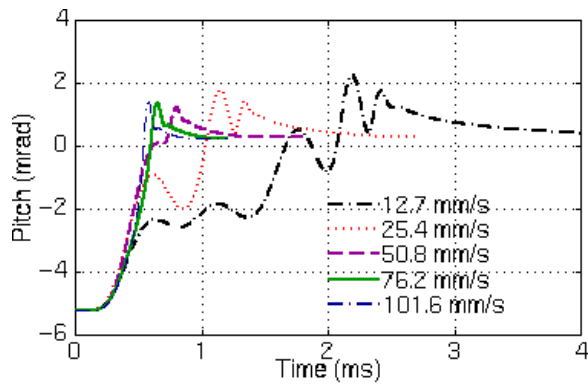


Fig. 5 Slider B's pitch and minimum clearance history for different disk RPM. (PSA=0.5 degree).



a) Slider A

b) Slider B

Fig. 6 Effects of the loading velocity (7200 RPM, 0 PSA, 30 μm initial FH)

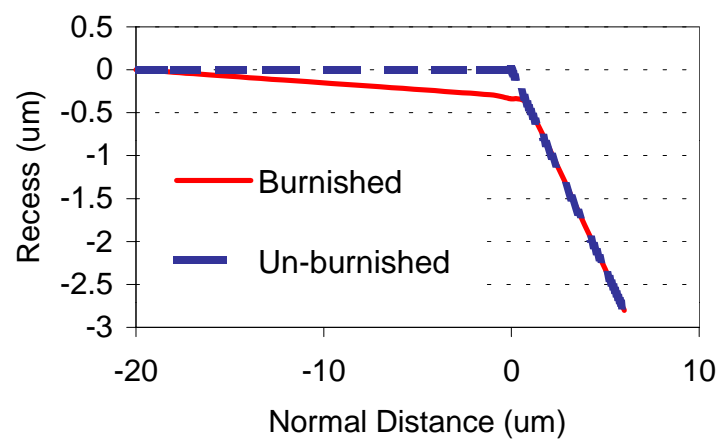
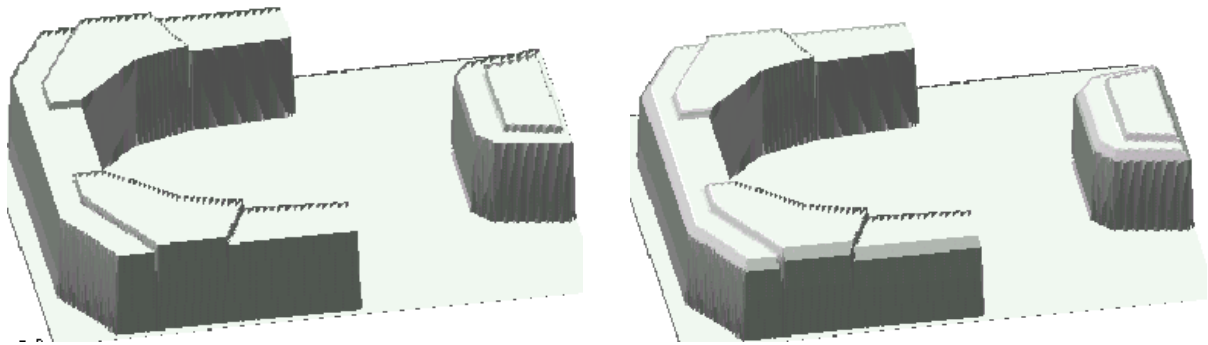


Fig. 7 Wall profiles of the sliders



a) Un-burnished

b) burnished

Fig. 8 The rail shapes of the slider before and after burnished

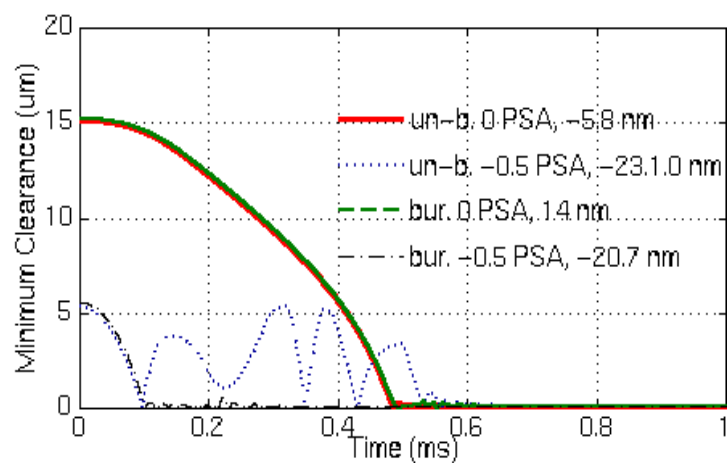
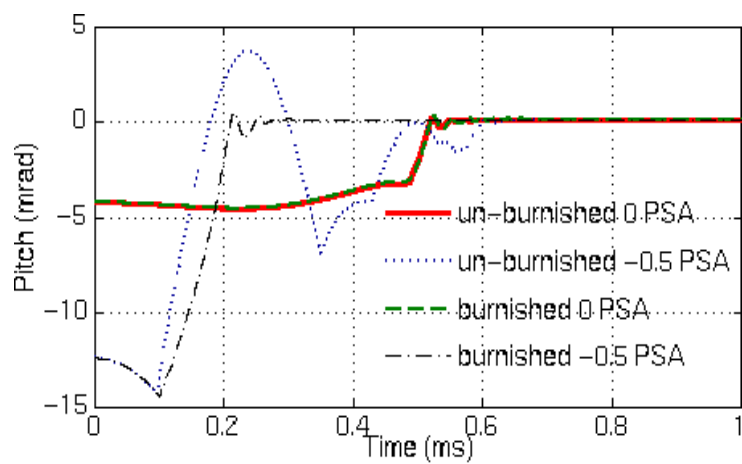


Fig. 9 Effects of slider burnish

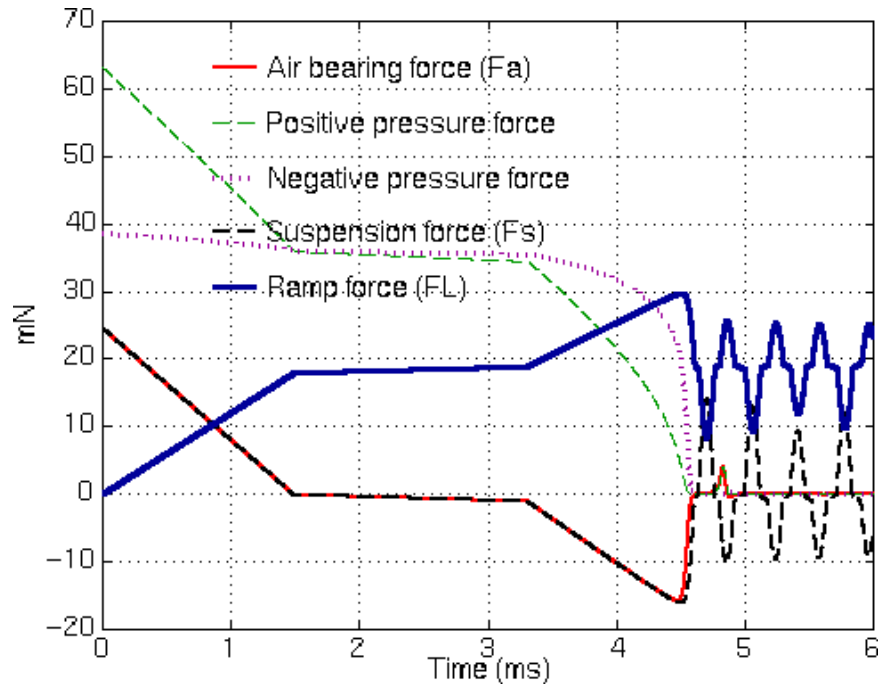


Fig. 10 Force histories of slider B unloaded at a 80 mm/s horizontal velocity (ramp A with a uniform 15 degrees slop)

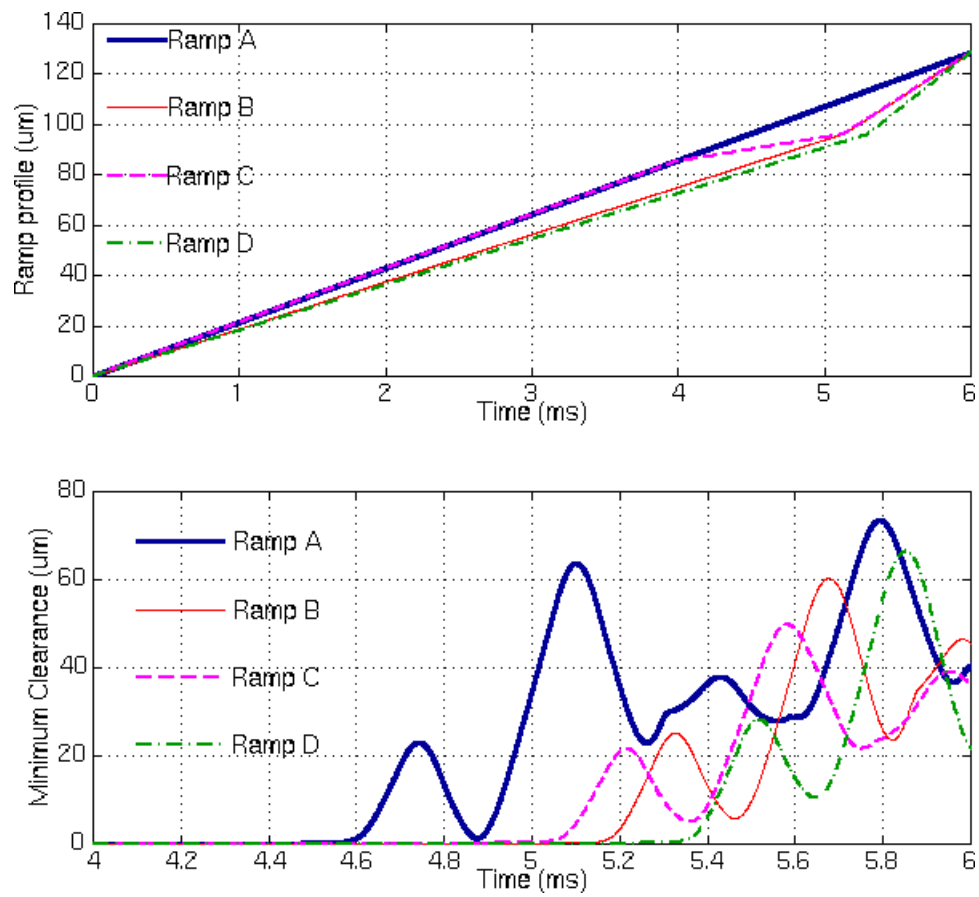


Fig. 11 Effects of ramp profile (unloading)

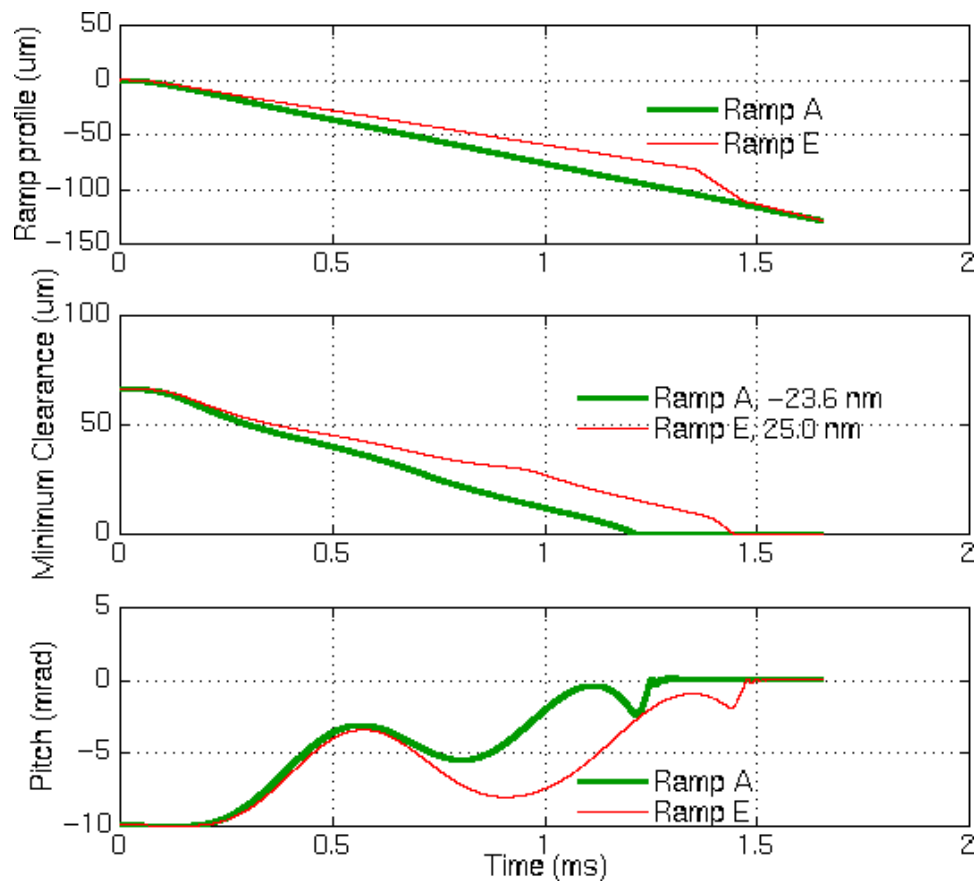


Fig. 12 Effects of ramp profile (high velocity loading)

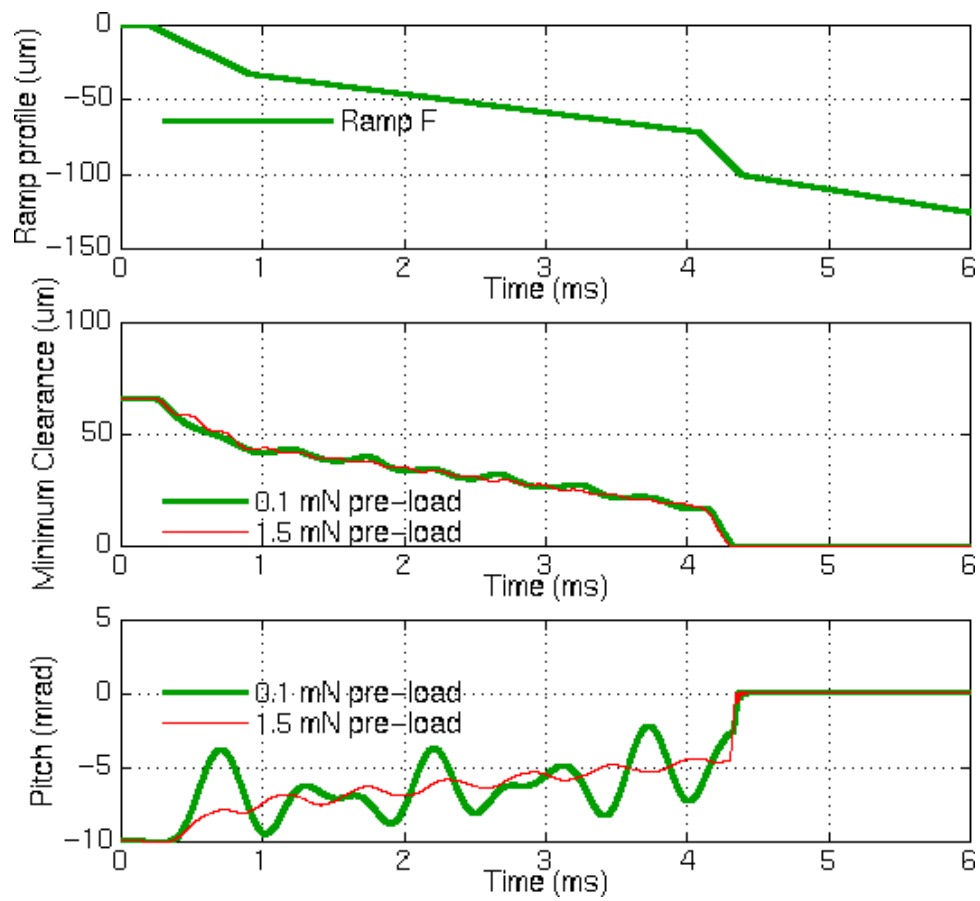


Fig. 13 Effects of dimple pre-load